catalysts

MDPI

Article

An Escape from Noble Metals for Generating Urethanes via Reductive Carbonylation of Nitroarenes over $FeSe_2/\gamma$-Al_2O_3 †

Anh Vy Tran [1], Thuy Tram Huynh Nguyen [1], Thanh Tung Nguyen [1], Hye Jin Lee [1], Jayeon Baek [2] and Yong Jin Kim [1,2,*]

1 Department of Green Process and System Engineering, Korea University of Science and Technology (UST), 89 Yangdaegiro-gil, Ipjang-myeon, Cheonan 31056, Korea; vybapcai@kitech.re.kr (A.V.T.); Thtr2602@gmail.com (T.T.H.N.); reymysterio.619.ntt@gmail.com (T.T.N.); master49@kitech.re.kr (H.J.L.)

2 Green Chemistry & Material Group, Korea Institute of Industrial Technology, 89 Yangdaegiro-gil, Cheonan-si 31056, Korea; jbaek@kitech.re.kr

* Correspondence: yjkim@kitech.re.kr; Tel.: +82-41-589-8469; Fax: +82-41-589-8580

† This article is based on a study first reported in Applied Catalysis A, General, 2019, 587, 117245.

Received: 14 September 2020; Accepted: 16 October 2020; Published: 22 October 2020



Abstract: The reaction of $FeCl_3$, SeO_2, and Pyridine (Py) in the presence of methanol (MeOH) under CO pressure generates a black precipitate, which has been confirmed as ferric di-selenide, $FeSe_2$ through different structure characterization methods. Furthermore, impregnation of 5 wt% of $FeSe_2$ onto γ-Al_2O_3 exhibits better catalytic performance than $FeSe_2$ due to the highly dispersed and smaller particle sizes ca. 200–300 nm. The reductive carbonylation of nitrobenzene (NB) was investigated over $FeSe_2/\gamma$-Al_2O_3 as a heterogeneous catalyst, delivering an excellent yield and high selectivity of methyl-*N*-phenyl carbamate (MPC). Moreover, a set of reactions was performed with variation in the reaction time, temperature, and pressure to investigate the effects of these factors. In particular, $FeSe_2/\gamma$-Al_2O_3 is highly stable and can be recycled for up to five cycles without significant loss in catalytic performance. A mechanistic study was also conducted on this low-cost catalyst system, especially proposing a crucial role of $FeSe_2$ (μ-CO) active species.

Keywords: ferrous selenide; nitrobenzene; reductive carbonylation; urethane

1. Introduction

Urethanes (carbamates) are essential precursors for producing isocyanates, the main material for manufacturing polyurethane, due to their transformation ability into isocyanates via thermal cracking. Conventionally, the production of urethanes involves the employment of phosgene, which is extremely toxic and harmful to the environment and human beings. Therefore, there have been tons of endeavors for producing carbamates via phosgene-free pathways [1–19]. Among them, the catalytic reductive carbonylation of nitroarenes is regarded as one of the promising routes [6–8,20–27]. Noble metal complexes containing Ru, Rh, and Pd have been commonly employed as main catalysts in this process [5,9,10,24,28–37]. Ragaini's research group showed that $[Pd(phen)_2][BF_4]_2$ could produce 71.05% yield of methyl-*N*-phenyl carbamate (MPC). In his work, the use of $[Pd(phen)_2][BF_4]_2$ resulted in ca. 6000 h^{-1} turnover frequency (TOF), which is the highest reported record to date [6,38]. Even though these catalyst systems showed high efficiency, there are still some limits in recyclability and leaching problems of noble metals-based catalysts. Meanwhile, selenium metal or selenium compounds have been widely used in catalytic reductive or oxidative carbonylation processes to produce carbamates from the corresponding aliphatic and aromatic amines. In the oxidative carbonylation of aromatic amine compounds, the active species were confirmed as Se(IV) such as SeO_2, $MSeO_3$, $MSeO_2(OR)$, $M_2Se_2O_5$,

and $QSeO_2(OR)$ (with M = alkali metal; Q = imidazolium, phosphonium) [1,2,39]; however, Se(0) is applied in reductive carbonylation [40–44]. Indeed, it has been reported that only Se(0) can convert nitrobenzene (NB) to urethanes and/or disubstituted ureas through reductive carbonylation [41,45].

Throughout our study on the reductive carbonylation of NB over different catalyst combinations consisting of Se-based and other metal halides to prepare MPC, we found that not only $Cu^{II}Se_2$, which has been already found by our research group as an active and novel heterogeneous catalyst [46], but also $Fe^{II}Se_2$ is found to be far more active than $Cu^{II}Se_2$ species. Like the case of $Cu^{II}Se_2$, the ferrous diselenide ($FeSe_2$) is also generated during the carbonylation reaction using the catalyst system consisting of $FeCl_3$ and SeO_2, but its activity was enhanced with the co-presence of pyridine. Additionally, $FeSe_2$ is a heterogeneous system that gives a simple separation and high selectivity toward urethanes. Furthermore, the catalyst can be prepared from the first-row transition metals, providing a promising route for replacing the precious metals in the reductive carbonylation of nitroarenes.

In this work, the authors provide the preparation of $FeSe_2$ and $FeSe_2/\gamma$-Al_2O_3 and characterization by various spectroscopic methods. Additionally, the catalytic activities of the $FeSe_2/\gamma$-Al_2O_3 in the reductive carbonylation will be investigated (Scheme 1). A plausible mechanism is also provided based on this active heterogeneous catalyst system, especially emphasizing the critical role of $FeSe_2(\mu$-CO) species.

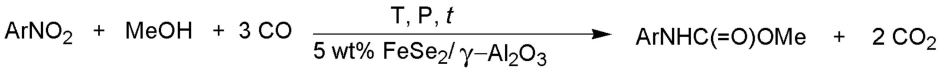

Scheme 1. The reductive carbonylation of nitroarenes over $FeSe_2/\gamma$-Al_2O_3.

2. Results and Discussion

2.1. Screening of the Catalyst Systems

The reductive carbonylation of NB for producing MPC was conducted over a catalyst system consisting of three compounds, $FeCl_3$, SeO_2, and pyridine (Py) in MeOH at 160 °C, 8.3 MPa of CO for 4 h. Table 1 shows that this catalyst combination generates MPC with a remarkable yield of 93.8% with complete conversion of NB (Entry 1). It is worth mention that the reductive carbonylation of NB is only effective when three components of $FeCl_3$, SeO_2, and Py are applied concomitantly. The absence of any components results in a decrease in the activities (Entry 2~4). Moreover, the single system (Entry 5~7) gives even worse outcomes. However, SeO_2 itself delivers 25.8% yield of MPC (Entry 6), (SeO_2 + Py), affording 37.8% (Entry 3), and ($FeCl_3$ + SeO_2) delivers 32.1% (Entry 2), demonstrating the importance of the presence of selenium in the reductive carbonylation. Furthermore, Se(0) itself could deliver 50.3% yield of MPC (Entry 8). Hence, 25.8% yield of MPC obtained from SeO_2 could be explained from an incomplete reduction of SeO_2 to Se(0) under this reducing conditions [41,42]. On the other hand, an insoluble solid was always formed during the reductive carbonylation of NB using the three-compound catalyst system. Being encouraged by this phenomenon, a reaction of $FeCl_3$ and SeO_2 in the methanolic Py solution is conducted without NB under otherwise identical conditions. After the reaction, the insoluble solid was collected by filtration, washed with methanol, and vacuum dried. The FT-IR results of this compound show there are no organic moieties; thus, it is thought to be an inorganic compound, and we tentatively named it as Fe_xSe_y.

Table 1. Screening of the catalysts system [a].

Entry	Catalyst Composition			NB Conv. (%)	MPC Yield (%)	AN Yield. (%)	TON
1	$FeCl_3$	SeO_2	Py	>99	93.8	6.2	11.7
2	$FeCl_3$	SeO_2	-	50.3	32.1	18.2	4.0
3		SeO_2	Py	46.5	37.8	8.7	4.7
4	$FeCl_3$	-	Py	0	0	0	0
5	$FeCl_3$	-	-	0	0	0	0
6	-	SeO_2	-	30.5	25.8	4.7	3.2
7	-	-	Py	0	0	0	0
8	-	Se^0	-	66.9	50.3	16.6	6.3

[a] Conditions: NB (2.46 g, 20 mmol), $FeCl_3$ (0.054 g, 0.4 mmol), SeO_2 (0.177 g, 1.6 mmol), Py (0.158 g, 2 mmol), molar ratio of NB/[Se] = 12.5, MeOH 30 mL, T = 160 °C, p_{CO} = 8.3 MPa, t = 4 h.

2.2. Characterization of Active Species and Its Supported System

Figure 1 shows that XRD spectra of Fe_xSe_y contains mainly ferroselite $FeSe_2$ phase [JCPDS 65-1455, Figure S1] [47,48]. To find out the stoichiometry of Fe_xSe_y, EDX/EDS analysis was carried out. The EDX/EDS spectra indicate the appearance of only Fe and Se, and Fe is combined with Se in the ratio of 1:2 (Supplementary Materials, Figure S3); thus, the stoichiometry of Fe_xSe_y is assumed to be $FeSe_2$.

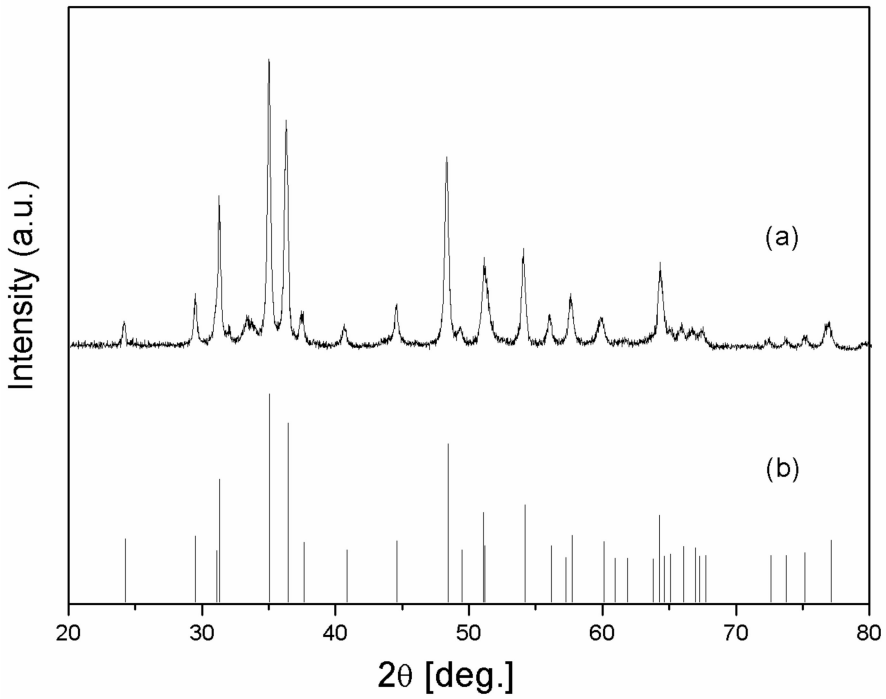

Figure 1. X-ray diffraction spectra (XRD) of (**a**) Fe_xSe_y, which is the black solid synthesized from the reaction of $FeCl_3$, SeO_2 in the presence of methanolic Py solution under CO pressure, and (**b**) standard pattern of ferroselite $FeSe_2$.

XPS analysis of $FeSe_2$ was conducted to examine the oxidation state of Fe and Se elements (Supplementary Materials, Figure S5). As shown in Figure S5, the XPS survey of $FeSe_2$ indicates that it comprises only Fe and Se. Furthermore, the Fe2p region depicted in Figure S7a shows that the band of Fe $2p_{1/2}$ and Fe $2p_{3/2}$ at 711.5 and 724.8 eV exhibits the presence of Fe^{2+} [49]. The minor peak at 707.1 eV is attributed to metallic $Fe^{0,}$ which could be resulting from the further reduction of Fe^{2+} to Fe^0 [49]. Meanwhile, the peak at 55.07 eV and 59.1 eV in Figure S7b belong to Se $3d_{5/2}$ and Se $3d_{3/2}$ of Se_2^{2-} species in $FeSe_2$ [49,50]. The C 1s XPS spectra was also investigated to check the formation of carbonaceous species of the sample. As can be seen in Figure S7c, the spectra did not exhibit the

presence of peaks belonging to carbonaceous compounds except the standard carbon peak at 284.8 eV for XPS calibration. These studies clearly demonstrate that the black compound generated during the reductive carbonylation is defined as ferrous diselenide ($Fe^{II}Se_2$).

The heterogeneous catalyst $FeSe_2$ was employed as the catalyst in the reductive carbonylation of NB for producing MPC. Table 2 reveals that $FeSe_2$ exhibits the best catalytic performance that shows 96.6% of MPC yield at the complete conversion of NB (Entry 1). After the reaction, aniline (AN, about 3.4%) was found as the only by-product, regarded as an intermediate in the reductive carbonylation of NB. Furthermore, when similar process is performed over $FeSe_2$, which was prepared without Py, the MPC yield is reduced to 85. 3%, suggesting the important role of Py, which is thought to render the particle size of the $FeSe_2$ smaller and uniformed (Entry 2). In comparison with the catalytic performance of other Se^{2-} species, a commercial chemical of $Fe^{II}Se$ was tested. However, it shows poorer activity in terms of both conversion and yield (Entry 3). A reported catalyst, $CuSe_2/CeO_2$ was also tested at the same conditions; however, it gives lower yield (63.5% yield of MPC at 68% conversion of NB) than that of $FeSe_2$ (Entry 9) [46].

Table 2. Activities of various MSe_2 and their supported systems [a].

Entry	Catalyst	Molar Ratio (NB/Cat)	NB Conv. (%)	MPC Yield (%)	AN Yield (%)	TON
1	$Fe^{II}Se_2$	4	>99	96.6	3.4	3.9
2 [b]	$Fe^{II}Se_2$	4	97.4	85.3	12.1	3.4
3	$Fe^{II}Se$	4	79.4	69.1	10.3	2.8
4	$Fe^{II}Se_2$	85	25.8	21.7	4.1	18.4
5 [c]	$FeSe_2/\gamma$-Al_2O_3	85	>99	98.9	1.1	84.1
6 [c]	$FeSe_2$/basic Al_2O_3	85	>99	91.6	8.4	77.9
7 [c]	$FeSe_2/\alpha$-Al_2O_3	85	98.1	87.8	10.3	74.6
8 [c]	$FeSe_2/AlPO_4$	85	87.0	85.7	1.3	72.8
9 [d]	$CuSe_2/CeO_2$	85	68	63.5	4.5	53.9

[a] Conditions: NB (2.46 g, 20 mmol), catalyst (5 mmol), molar ratio of NB/catalyst = 4, MeOH (30 mL), T = 160 °C, P (CO) = 8.3 MPa, t = 4 h. [b] NB (2.46 g, 20 mmol), $Fe^{II}Se_2$ synthesized without Py (1.07 g, 5 mmol), MeOH (30 mL), T = 160 °C, P (CO) = 8.3 MPa, t = 4 h. [c] NB (2.46 g, 20 mmol), 4~5 wt% $FeSe_2$/support (1 g, [$FeSe_2$]: 0.2338 mmol), molar ratio of NB/$FeSe_2$ = 85, MeOH (30 mL), T = 160 °C, P (CO) = 8.3 MPa, t = 4 h. [d] NB (2.46 g, 20 mmol), 4~5 wt% $CuSe_2/CeO_2$ (1.04 g, [$CuSe_2$]: 0.235 mmol). Molar ratio of NB/$CuSe_2$ = 85, MeOH (30 mL), T = 160 °C, P (CO) = 8.3 MPa, t = 4 h.

From these observations, it is concluded that Se_2^{2-} is the most responsible species for providing high activity toward MPC, and this trend is significantly noticeable when using ferrous diselenide ($FeSe_2$).

To enhance the catalytic performance of $FeSe_2$ by an impregnation approach, a wet impregnation technique has been adopted with different types of supports such as γ-Al_2O_3, basic Al_2O_3, α-Al_2O_3, and $AlPO_4$ with 5 wt% of $FeSe_2$ loadings. As shown in entries from 5 to 9 in Table 2, γ-Al_2O_3 supported $FeSe_2$ exhibits the highest catalytic activity toward MPC (98.9% yield, Entry 5). It is noteworthy to mention that the molar ratio of NB/$FeSe_2$ of this reaction over $FeSe_2/\gamma$-Al_2O_3 is almost twenty times higher than that of the neat $FeSe_2$ in terms of the molar ratio basis (Entry 1), indicating that the catalytic performance of $FeSe_2/\gamma$-Al_2O_3 was enhanced without any loss of selectivity. Indeed, the MPC yield when using neat $FeSe_2$ at the same molar ratio of 85 is found to be very low (21.7%, Entry 4). Basic Al_2O_3, α-Al_2O_3, and $AlPO_4$ did not show as good activity as γ-Al_2O_3 (entries 6~8), and activities of other supporting materials are also provided in the Supplementary Materials (Table S1), and XRD results of $FeSe_2/\gamma$-Al_2O_3 and its XPS spectra are presented therein (Figures S2 and S6).

To examine the role of Py, the possible correlation between morphologies and activities of the catalysts was studied using SEM image and MPC yields. As shown in Figure 2, $FeSe_2$ synthesized without Py exhibits the irregular rod-typed morphology, whereas the one made with Py exhibits the identical flake typed and well-dispersed morphologies. The observed size of $FeSe_2$ without Py is about

1–1.1 μm (Figure 2a), while that of $FeSe_2$ prepared with Py decreased to ca. 400–450 nm (Figure 2c). The catalytic activity is also correlated with the size of catalysts, that is, the smaller the particle size, the better the performance on the formation of MPC (see Table 3). When we compare the SEM images of the supported system, $FeSe_2/\gamma$-Al_2O_3 prepared without Py shows irregular rod and flake typed structures with a size of 0.75 μm (Figure 2b). However, $FeSe_2/\gamma$-Al_2O_3 prepared with the presence of Py exhibits regular and well-dispersed particles of 200–300 nm (Figure 2d), almost two times smaller than the prepared with Py without the support. These results indicate that the presence of Py helps to render the size of $FeSe_2$ regular and smaller. Therefore, it is concluded that the improvement of catalytic activity in the $FeSe_2/\gamma$-Al_2O_3 system is attributed to the higher dispersion of $FeSe_2$ particles onto γ-Al_2O_3. High-resolution TEM images of $FeSe_2$ and $FeSe_2/\gamma$-Al_2O_3 are also provided in Figure S9.

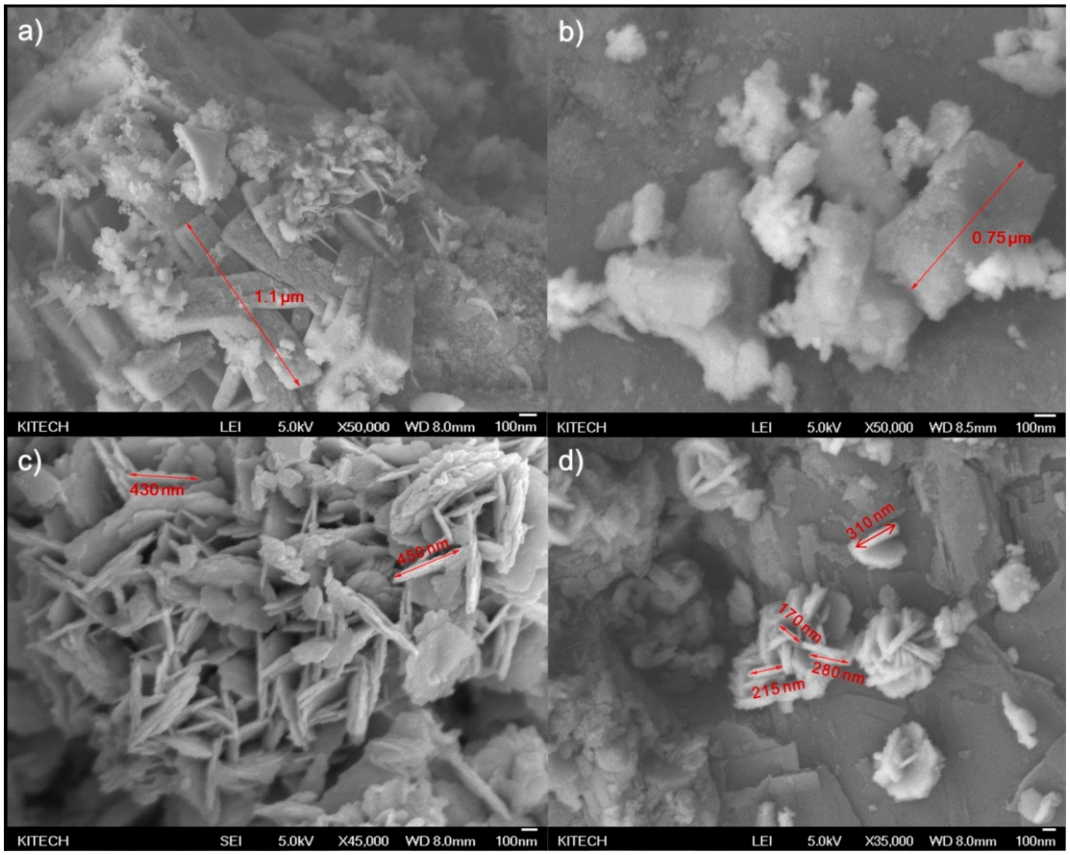

Figure 2. Scanning Electron Microscopy (SEM) images of (**a**) $FeSe_2$ prepared without pyridine, (**b**) $FeSe_2/\gamma$-Al_2O_3 prepared without pyridine, (**c**) $FeSe_2$ prepared with pyridine, and (**d**) $FeSe_2/\gamma$-Al_2O_3 prepared with pyridine.

Table 3. Correlation between morphologies and activities [a].

Entry	Catalyst	Molar Ratio (NB/Cat)	NB Conversion (%)	MPC Yield (%)	Morphology	Size
1	$FeSe_2$ without Py	4	97.4	85.3	Irregular rod-type and aggregated flakes	1–1.1 μm
2	$FeSe_2$ with Py	4	>99	96.6	Uniformed flake-type	400–450 nm
3 [b]	$FeSe_2/\gamma$-Al_2O_3 without Py	85	78.7	73.8	Irregular rod-type	0.7–0.75 μm
4 [b]	$FeSe_2/\gamma$-Al_2O_3 with Py	85	>99	98.9	Uniformed flake-type dispersed on support	200–300 nm

[a] Conditions: NB (2.46 g, 20 mmol), $FeSe_2$ (1.01 g, 5 mmol), molar ratio of NB/$FeSe_2$ = 4, MeOH (30 mL), T = 160 °C, P (CO) = 8.3 MPa, t = 4 h. [b] NB (2.46 g, 20 mmol), 5 wt% $FeSe_2/\gamma$ -Al_2O_3 (1 g, [$FeSe_2$]: 0.2338 mmol), molar ratio of NB/$FeSe_2$ = 85, MeOH (30 mL), T = 160 °C, P (CO) = 8.3 MPa, t = 4 h.

2.3. Catalytic Activities of $FeSe_2/\gamma$-Al_2O_3

To investigate product profile as a span of reaction time in the reductive carbonylation of NB over $FeSe_2/\gamma$-Al_2O_3, a set of experiments was conducted with variable reaction time ranging from 0.5 h to 6.0 h. The results illustrated in Figure 3 show that the amount of MPC arises upon elevating time from 0.5 to 4 h and then keeps constant. Upon prolonging the time to 4 h, the amount of NB reduced rapidly. Moreover, this time-course study also shows that aniline (AN) is the only by-product during the conversion of NB, and it is suppressed within 0.14 mmol level.

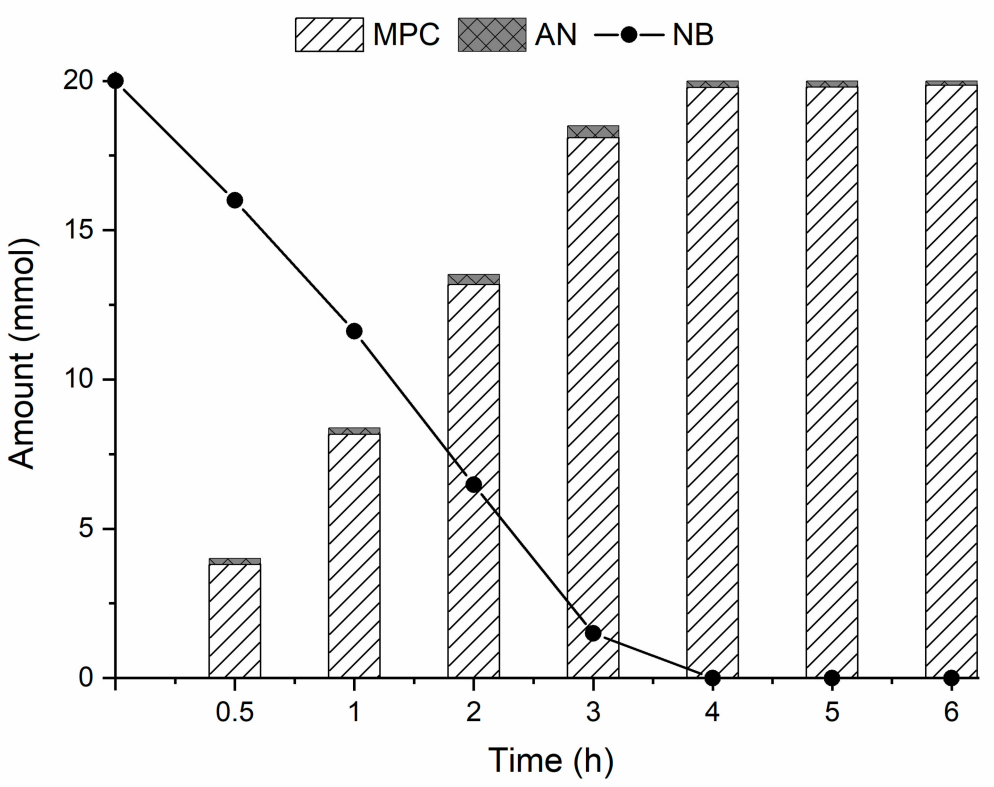

Figure 3. Product compositional changes as a function of time in the reductive carbonylation of NB at 160 °C, 8.3 MPa of CO in the presence of 1 g of 5 wt% $FeSe_2/\gamma$-Al_2O_3. Conditions: NB (20 mmol), 5 wt% $FeSe_2/\gamma$-Al_2O_3 (1 g, [$FeSe_2$]: 0.2338 mmol), molar ratio of NB/$FeSe_2$ = 85, MeOH (30 mL), T = 160 °C, p = 8.3 MPa of CO.

The influence of the reaction temperature on the reductive carbonylation of NB over $FeSe_2/\gamma$-Al_2O_3 was tested with a variable thermal scale from 120–180 °C. As shown in Figure 4, the higher MPC yield was obtained when elevating the temperature until 160 °C, thereafter both conversion and yield are decreased. The generation of AN could not be neglected at a low temperature of 120 °C, which is ascribed to a simple reduction of NB to AN. However, AN reduces with a further increase in the temperature up to 160 °C. The lower yield of MPC, together with the increase in the aniline (AN) formation at 180 °C might be due to the thermal decomposition of MPC.

The influence of CO pressure was also studied by elevating pressure from 6.2 to 10.3 MPa at 160 °C for 4 h. As shown in Figure 5, the results reveal that the pressure effect is not as strong as the reaction temperature; however, at least 6.8 MPa of CO is needed to achieve an acceptable MPC yield. It is worth mentioning that the AN formation is suppressed with the increase in the pressure, suggesting that the high pressure of CO is beneficial for the generation of selenium-carbonyl species which might act as an intermediate.

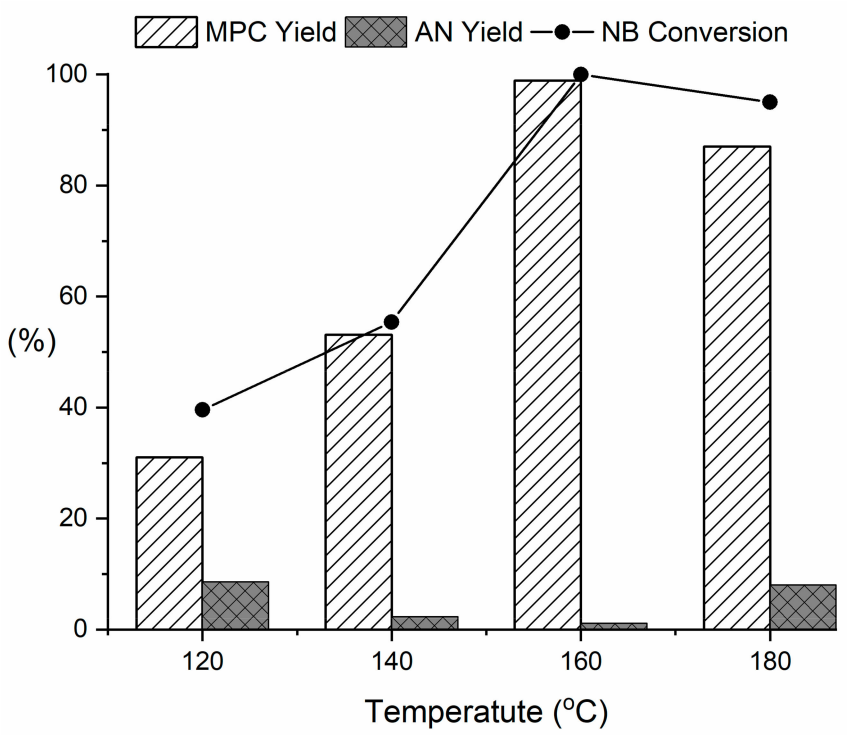

Figure 4. Effect of temperature on the formation of MPC at 8.3 MPa of CO for 4 h in the presence of 1 g of 5 wt% $FeSe_2/\gamma$-Al_2O_3. Conditions: NB (20 mmol), 5 wt% $FeSe_2/\gamma$-Al_2O_3 (1 g, [$FeSe_2$]: 0.2338 mmol), molar ratio of NB/$FeSe_2$ = 85, MeOH (30 mL), p = 8.3 MPa of CO, t = 4 h.

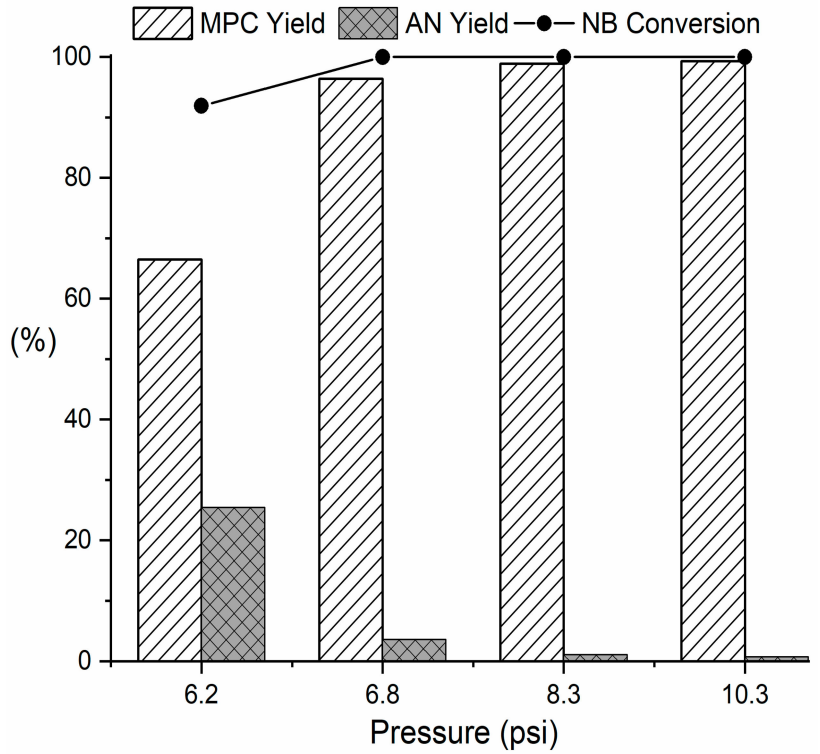

Figure 5. Effect of pressure on the formation of MPC at 160 °C for 4 h in the presence of 1 g of 5 wt% $FeSe_2/\gamma$-Al_2O_3. Conditions: NB (20 mmol), 5 wt% $FeSe_2/\gamma$-Al_2O_3 (1 g, [$FeSe_2$]: 0.2338 mmol), molar ratio of NB/$FeSe_2$ = 85, MeOH (30 mL), T = 160 °C, t = 4 h.

To broaden the scope of applicability of the $FeSe_2/\gamma$-Al_2O_3-catalyzed reductive carbonylation, different nitroaromatic compounds were applied as substrates under 160 °C, 8.3 MPa for 4 h (hereafter these conditions will be regarded as standard conditions). As demonstrated in Table 4, 4-nitroanisole having an electron-donating group (EDG) at para position is transformed to methyl-*N*-4-methoxyphenyl) carbamate with very high yield (98.5%, Entry 1), while 4-nitrotoluene and 4'-nitroacetophenone is converted to the corresponding carbamates only in 50.1% and 48% yields, respectively (Entry 3 and 4). Additionally, 3-nitroanisole, bearing (EWG) at the meta-position, was transformed to the corresponding carbamate in lower yield (80%, Entry 2). When it was carried out with 4-bromonitrobenzene with an electron-withdrawing group (EWG) at the para position, carbamate yield dropped significantly to 19.7%. These results imply that the EDG/EWG capability of the substituents might affect the catalytic performance of the reductive carbonylation of nitroarenes, i.e., the presence of electron-withdrawing group at the para position tended to reduce the catalyst activity of the carbonylation reaction. The 2,4-dinitrotoluene (2,4-DNT), a main precursor for manufacturing toluene diisocyanate (TDI), is also converted to the corresponding dicarbamate, but the yield was 41.5% even at higher temperature (180 °C), longer reaction time (6 h), and higher catalyst amount (molar ratio of sub/cat = 42), (Entry 6). Surprisingly, the carbonylation of 1,4-nitroaniline gives 40.5% yield of the corresponding diurethane under the optimized conditions. Being encouraged by this outcome, a set of experiments has been conducted by adding a variety amount of aniline (AN) with varying from 20% to 200% based on NB (mol/mol). Figure 6 shows that the MPC yield dramatically increases upon adding AN with 180% (substrate: NB 10 mmol and AN 18 mmol) then reduces. The highest yield of MPC is 204% based on NB, which is almost two times higher than that in the case of without AN. The positive effect of adding AN in the reductive carbonylation has been reported, and it accelerates the reductive carbonylation reaction of NB over a palladium-phenanthroline catalyst system [51]; however, this protocol eventually gave rise to a decrease in the selectivity due to the generation of large amounts of azoxybenzene [6]. Nevertheless, the $FeSe_2/\gamma$-Al_2O_3 catalyst did not show any azoxybenzene as a side-product.

The additional formation of MPC by adding AN can be rationalized by the following in situ cascade reactions: (i) a reaction between AN and isocyanato species produces diphenyl urea (DPU), then (ii) methanolysis of DPU affords MPC (*2.5. Mechanism study*). This is fairly acceptable because a quantitative production of MPC was verified from the alcoholysis of DPU by methanol in the absence of a catalyst.

It should be clear that the MPC was not obtained when AN was used as a sole substrate (Table 4, Entry 11), which indicates that AN itself cannot be carbonylated or work as an intermediate in the reductive carbonylation over $FeSe_2$ for producing MPC. On the other hand, AN works as a reactant for the generation of DPU via in situ reaction with an isocyanato intermediate, which might be a reasonable explanation about the high reactivity of nitroaniline in the $FeSe_2$-catalyzed reductive carbonylation. To confirm this, a reductive carbonylation over 5 wt% $FeSe_2/\gamma$-Al_2O_3 (1 g, with a molar ratio of sub/cat = 170) was conducted by employing the dual substrates system consisting –nitro (20 mmol) and –amino (20 mmol) substrate bearing the same functional group at the para-position of the aromatic ring under standard conditions. After the reaction, the corresponding urethanes were generated in 148.4 and 161.1% yields based on nitro substrate, respectively (Entries 8 and 9, Table 4), which are 1.5 and 3.2 times higher than in the case of the sole substrate system (Entry 1 and 3, Table 4). Moreover, a dual substrates 2,4-dinitrotoluene and 2,4-diaminotoluene were also applied for the reductive carbonylation, catalyzed by only 1 g of $FeSe_2/\gamma$-Al_2O_3 (sub/cat molar ratio = 170) under the standard conditions. Interestingly, the di-carbamate yield was found to be 92.5% (Entry 10, Table 4). Compared to the yield of the nitro substrate (41.5%) at a longer reaction time (6 h), higher temperature (180 °C), and higher catalyst amount, the catalytic performance of this dual substrate system in the standard conditions can be regarded as astonishing.

Table 4. Reductive carbonylation of various nitro compounds [a].

Entry	Substrates		Product	Conv. (%)		Yield (%)
	Nitro	Amino		Nitro	Amino	
1	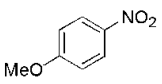		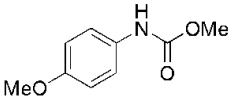	>99		98.5
2	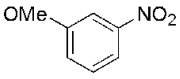		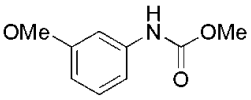	92.5		80.0
3	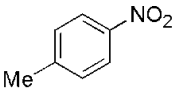		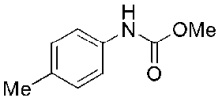	56.4		50.1
4	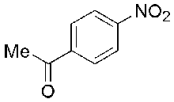		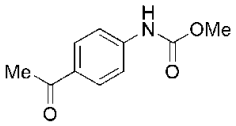	50.5		48.0
5	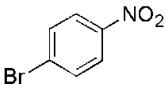		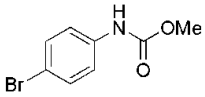	35.5		19.7
6 [b]	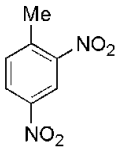		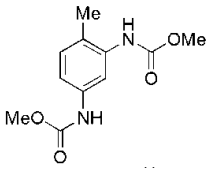	> 99		41.5
7	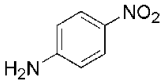		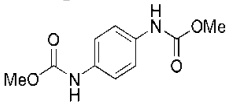	98.5		40.5
8 [c]	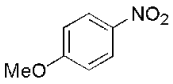	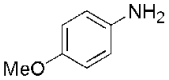	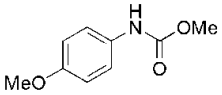	87.2	90.0	148.4
9 [c]	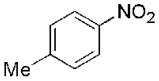	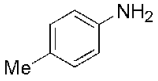	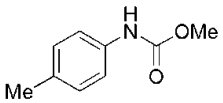	99.5	74.2	161.1
10 [c]	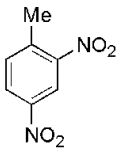	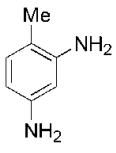	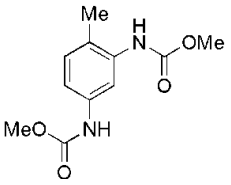	>99	>99	92.5
11	Aniline		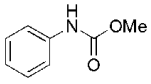	NR		0

[a] Conditions: Substrate (20 mmol), 5 wt% $FeSe_2/\gamma$-Al_2O_3 (1 g, [$FeSe_2$]: 0.2338 mmol), molar ratio of sub/$FeSe_2$ = 85, MeOH (30 mL), T = 160 °C, P (CO) = 8.3 MPa, *t* = 4 h. [b] Substrate (10 mmol), 5 wt% $FeSe_2/\gamma$-Al_2O_3 (1 g, [$FeSe_2$]: 0.2338 mmol), molar ratio of sub/$FeSe_2$ = 42, MeOH (30 mL), T = 180 °C, P (CO) = 8.3 MPa, *t* = 6 h. [c] Nitro compound (20 mmol), aniline compound (20 mmol), 5 wt% $FeSe_2/\gamma$-Al_2O_3 (1 g, [$FeSe_2$]: 0.2338 mmol), molar ratio of (nitro + aniline)/$FeSe_2$ = 170, MeOH (30 mL), T = 160 °C, *p* (CO) = 8.3 MPa, *t* = 4 h.

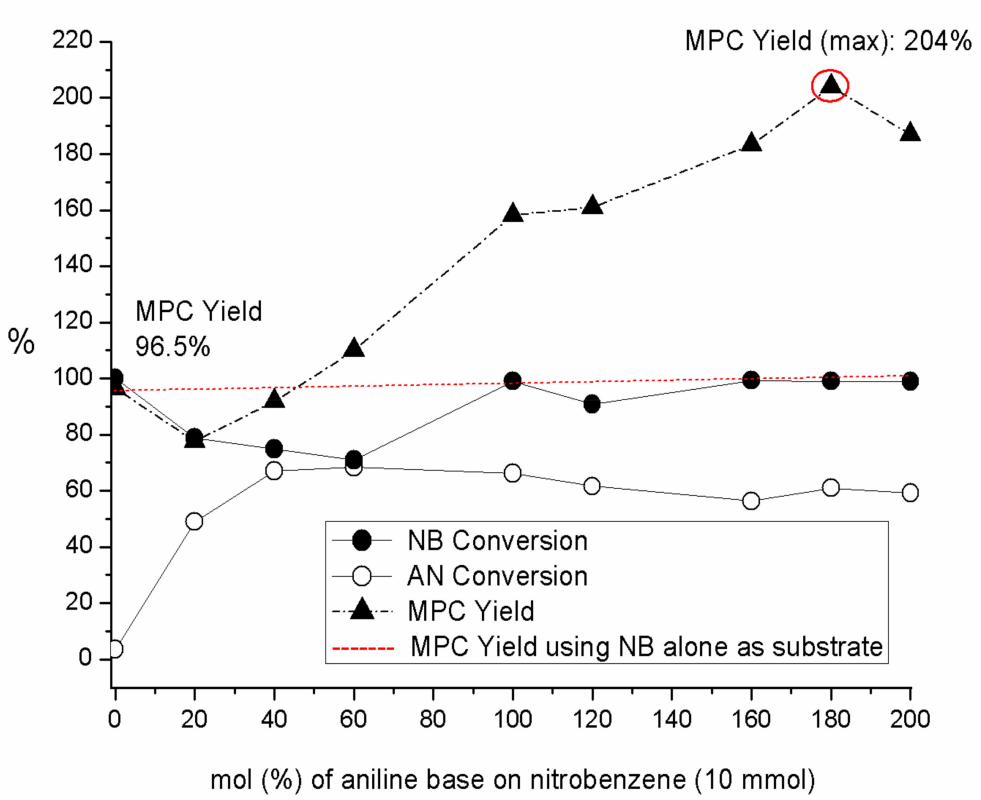

Figure 6. Effect of the addition of aniline on the activity of the reductive carbonylation of nitrobenzene. Conditions: NB (10 mmol), 5 wt% $FeSe_2/\gamma$-Al_2O_3 (0.5 g, [$FeSe_2$]: 0.1169 mmol), molar ratio of NB/$FeSe_2$ = 85, MeOH (30 mL), T = 160 °C, p = 8.3 MPa of CO, t = 4 h.

2.4. Catalyst Recyclability

To investigate the reusability of $FeSe_2/\gamma$-Al_2O_3, a set of experiments was conducted under milder conditions, that is, 140 °C (original temperature was 160 °C), under 6.8 MPa of CO pressure (original 8.3 MPa) for 2 h (original 4 h), and using 1.0 g of $FeSe_2/\gamma$-Al_2O_3 (molar ratio of NB/[$FeSe_2$] = 85) to exclude the effects of high temperature and pressure as well as long reaction time that could maintain high yield of MPC in every cycle. After reaction for 2 h, the solid $FeSe_2/\gamma$-Al_2O_3 was filtered and washed with methanol, vacuum dried overnight, and recycled for the subsequent reaction with newly charged NB. The results illustrated in Figure 7 indicate that $FeSe_2/\gamma$-Al_2O_3 did not show any loss in the catalytic activity until three consecutive recycles; however, there seems to be a small loss in the activity from the 4th recycling, implying that this low-cost heterogeneous $FeSe_2/\gamma$-Al_2O_3 is fairly recyclable. Furthermore, the XRD result of the used catalyst depicted in Figure S22 shows that the diffraction patterns maintained their initial 2-theta value and intensity, demonstrating there is no change in the structure of this catalyst. Furthermore, no remarkable differences in the morphology after the reaction (Figure S21). To examine the change in the oxidation state of the used catalyst, XPS analysis was conducted. As shown in Figure S23, the reused catalyst shows a small shift in the Se 3d region from 54.57 eV to 55.3 eV, implying a partial generation of Se (0) species during reductive carbonylation, which is in high agreement with the generation of the Se^0-CO as observed using IR analysis (Figure 8), while the oxidation state of Fe did not change. These phenomena will be described in more detailed in the Section 2.5. The possible leaching of ferric or selenium elements was investigated by examining the liquid phase after the reaction using the ICP-MS method. The results show that there are no leached selenium species, indicating that $FeSe_2/\gamma$-Al_2O_3 is a highly robust heterogeneous catalyst.

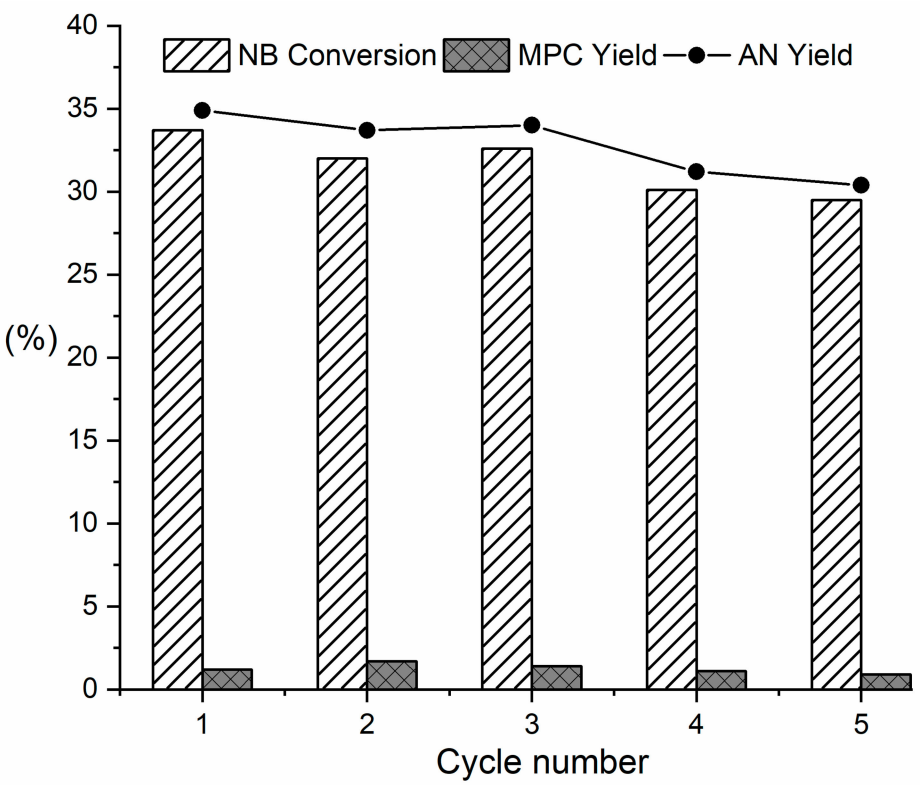

Figure 7. Catalyst recyclability in the reductive carbonylation of NB at 140 °C, 6.8 MPa of CO for 2 h in the presence of 1 g of 5 wt% $FeSe_2/\gamma$-Al_2O_3.

2.5. Mechanism Study

To determine the active species of the reductive carbonylation, $FeSe_2$ was reacted with CO (8.3 MPa) in the presence of methanol at 160 °C for 4 h. The resulting solids were collected and dried under vacuum, and then pelletized with KBr. The sample was analyzed by FT-IR spectroscopy, but no carbonyl band of $FeSe_2$ was observed (Scheme 2, Figure 8a). On the other hand, when the same process was carried out in the presence of O_2 with CO, i.e., CO/O_2 mixture (*v*/*v* = 80:20) (Scheme 3), FT-IR spectra of this sample exhibits a carbonyl peak at 1796 cm^{-1} (Figure 8b).

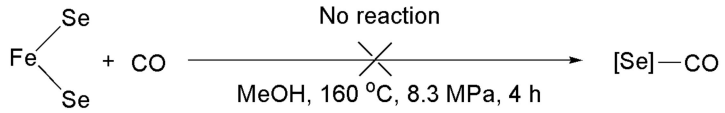

Scheme 2. The reaction of $FeSe_2$ and CO in the presence of methanol at 160 °C for 4 h.

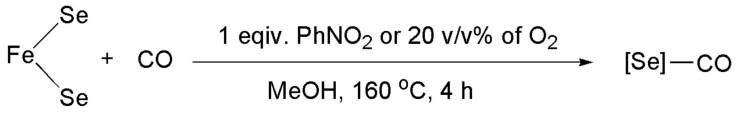

Scheme 3. The reaction of $FeSe_2$ and CO in the presence of oxidant.

As CO does not tend to bind to Fe(II), it might be bound to Se(0) in $FeSe_2$, which demonstrates that the carbonyl species binds through Se, then forms carbonyl $FeSe_2$ is possible only when Se^- is oxidized to Se^0 in the presence of an oxidant ($Se^{-1} \rightarrow Se^0$). In this $FeSe_2$-catalyzed reductive carbonylation, NB contributes as an oxidant. Indeed, the IR experiment conducted on a sample treated in the existence of NB (1 equiv. to $FeSe_2$) under CO pressure in the absence of oxygen also exhibits the CO band at the same wavelength (Figure 8c). These spectroscopic observations suggest that some part of the Se^- species in $FeSe_2$ seems to be oxidized to pseudo-Se(0), and is then partially converted to Se-CO moiety.

In consideration of the fact that the synthesis of the terminal (Se-CO) proceeds in severe conditions such as metal Se reacting with carbon monoxide at 500–700 °C [52] or the reaction between phosgene and Al_2Se_3 at 210 °C [53], the clear observation of Se-CO species using $FeSe_2$ seems to be very encouraging. In fact, Sonoda et al. reported the vapor phase of prepared Se-CO at ambient condition. Furthermore, the Se-CO was prepared by using distillation at −50 °C/5 torr, then cooling at −196 °C by introducing ammonium selenocarbamate into the mixture of THF/strong acid at −78 °C [54]. Bearing in mind these facts, it seems that the CO peak obtained at 1796 cm^{-1} from the IR result could be ascribed as bridging structure. Based on the well-known fact that the IR stretching vibration of the terminal Se-CO as a vapor phase is around 2009 cm^{-1} [55], and the IR spectra of CO stretching vibration as bridging form fall to 1720–1850 cm^{-1} [56], the CO peak at 1796 cm^{-1} can be defined as bridging form.

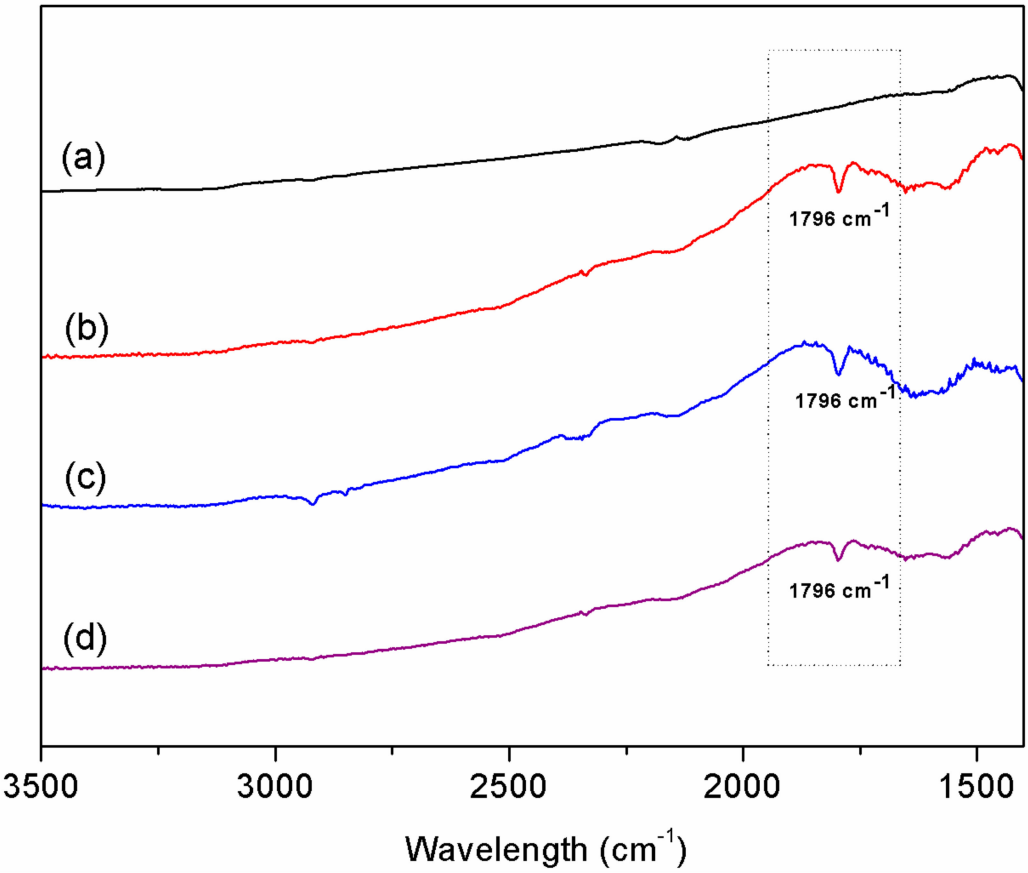

Figure 8. FT-IR spectra of (**a**) $FeSe_2$ obtained from the reaction with CO only, (**b**) $FeSe_2$ obtained from the reaction in CO/O_2 gas mixture (*v*/*v* = 80:20), (**c**) $FeSe_2$ obtained from the reaction with CO by adding NB as oxidant, (**d**) spent $FeSe_2$ after the carbonylation reaction.

Scheme 7 provides a plausible mechanism of the reductive carbonylation of nitroarene catalyzed by $FeSe_2$. The first step of the carbonylation would be the reaction of $FeSe_2$ with methanol to form (**1a**) (Scheme 4), then the generation of active catalyst, $FeSe_2$(μ-CO) (**1b**) via the reaction between **1a** and CO in the presence of NB. Once again, it is worth emphasizing that **1b** is not able to generate by the direct reaction between $FeSe_2$ and carbon monoxide (Scheme 2) without the presence of an oxidant like oxygen or NB, as studied using FT-IR analysis (Figure 8). The combination of Schemes 4 and 5 generates Scheme 6, indicating that the formation of $FeSe_2$(μ-CO) (**1b**) can be assisted by the conditions of the reductive carbonylation of NB.

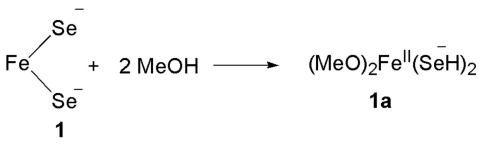

Scheme 4. The reaction of $FeSe_2$ with methanol for producing **1a**.

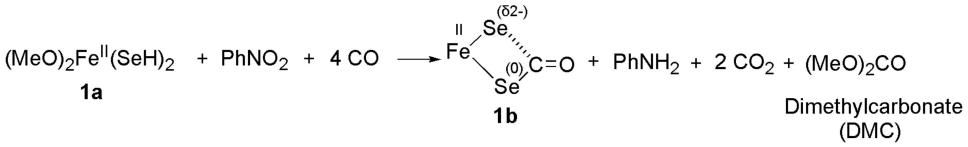

Scheme 5. The generation of **1b** via the reaction of **1a** with CO in the presence of NB.

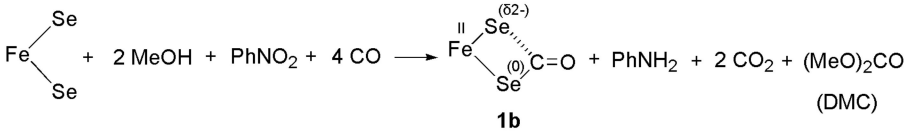

Scheme 6. The combination of Schemes 4 and 5.

Although it was not successful in observing **1a** by reacting $FeSe_2$ with MeOH even for a longer time (overnight), the observation of AN and dimethyl carbonate (DMC) was confirmed through GC-MS analysis, as shown in Scheme 6 (SI, Figure S11). Meanwhile, Cotton reported the semi-bridging carbonyl with the CO group is an intermediate between terminal and bridging form [57]. The suggested structure of $FeSe_2$(μ-CO) (**1b**) is proposed as semi-bridging carbonyl as well, where the μ-CO is bound asymmetrically to two Se. The length of Se(δ^{2-})–CO bond might be longer than that of Se(0)–CO, allowing the insertion of NB between Se and carbonyl carbon to be more comfortable through comparatively weaker interaction. Therefore, the reaction of **1b** with NB will form **2b** via the weaker bond, followed by subsequent decarboxylation (-CO_2) to generate **3b**. Then, one CO will be inserted between Se and O bond to generate **4b**, and the second decarboxylation will produce a ferrous diselenide nitrido moiety, **5b**. The formation of **5b** is very important, because it is well known as the formation of L_nM = NR in the noble metal-catalyzed reductive carbonylation of nitroarenes [7] This is due to the labile property that can be converted to other compounds such as isocyanates, carbamates, amines, and ureas [7,13,23,24]. Next, **5b** is carbonylated with another CO to produce an isocyanato species, **6b**. In the end, **6b** can aggressively react with methanol to generate urethane with simultaneous regeneration of **1b**. We should mention, here, the reason for the noticeable enhancement in the carbamates productivity by employing corresponding amino compounds into the nitro substrate. It can be understood as follows: (i) **6b** interacts with RNH_2 to produce disubstituted urea (DSU, $(RNH)_2CO$, (ii) DSU will be transformed into carbamate and amine via methanolysis, and (iii) the produced amino compound takes part in this small repeated cycle, resulting in an additional generation of carbamates (solid box in Scheme 7).

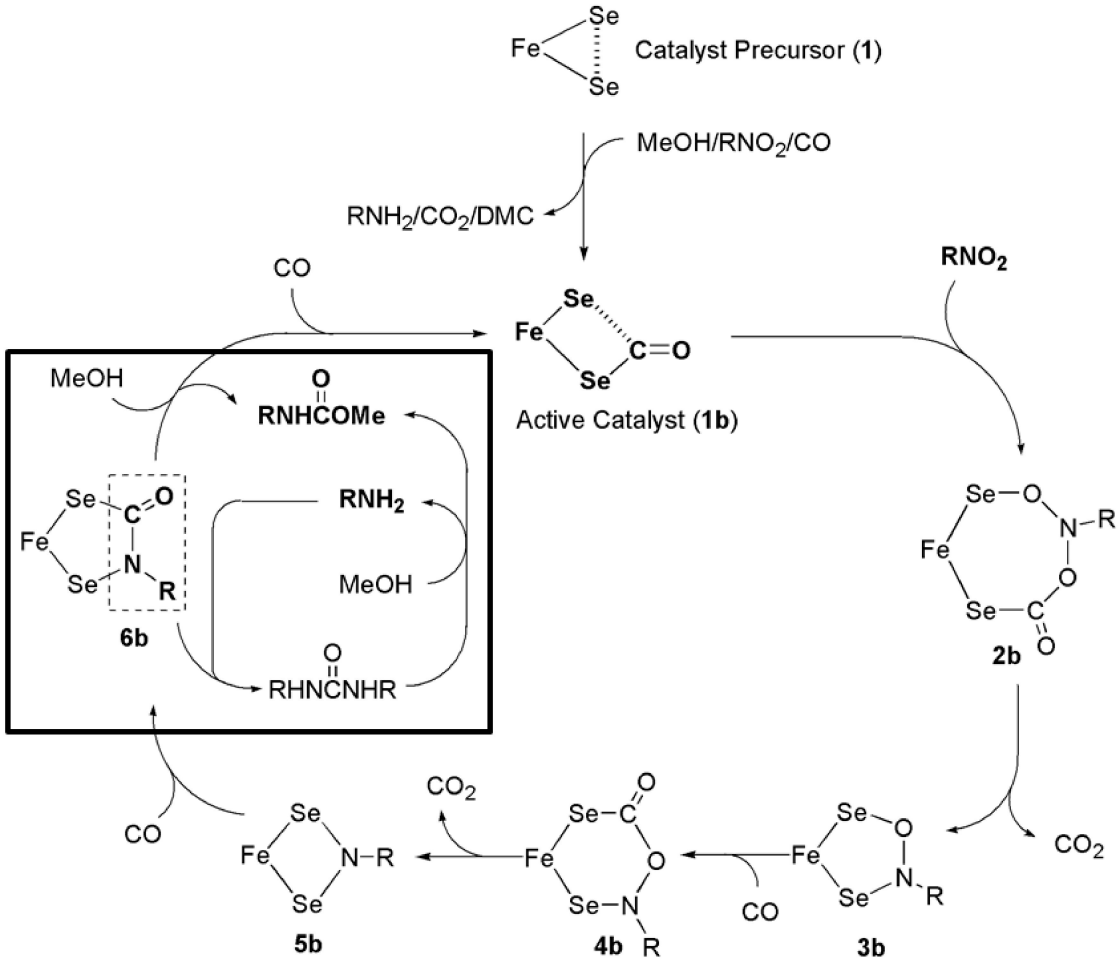

Scheme 7. Plausible mechanism of $FeSe_2$-catalyzed reductive carbonylation of nitroarene to produce urethane. The solid box explains about the enhanced urethane productivity when adding corresponding amino compound to the nitro compound-based main catalytic cycle.

3. Experimental

3.1. Materials

All chemicals, including iron (III) chloride ($FeCl_3$, 97%), selenium dioxide (SeO_2, 98.0%), pyridine (Py > 99.0%), and nitrobenzene (NB ≥ 99.0%), were purchased from Sigma-Aldrich (St. Louis, MO, USA). The support γ-Al_2O_3 (99.97%), α-alumina (α-Al_2O_3, 99.9%), basic-Al_2O_3 (99.8%), and neutral-Al_2O_3 (99.9%) were obtained from Alfa-Aesar (Ward Hill, MA, USA). Nitrobenzene (NB) and MeOH were freshly distilled under atmosphere of nitrogen. CO with 99.95% purity was supplied from Uniongas (Seoul, South Korea) and without further purification.

3.2. Catalyst Characterization

The surface structure of $FeSe_2$/γ-Al_2O_3 was examined by using scanning electron microscopy (SEM, JEOL JSM-6701F) and transmission electron microscopy analysis [TEM, JEM-2100F (UHR)]. The elemental compositions of catalysts were investigated by the associated EDX system (INCA). The oxidation states of each element on the surface of $FeSe_2$ and its supports were examined by X-ray photoelectron spectroscopy (XPS) analysis on the Thermo Scientific K-Alpha^{TM+} spectrometer (Thermo Fisher Scientific Korea Ltd., Seoul, South Korea). X-ray diffraction (XRD) studies were analyzed on the Bruker D8 Advance (Waltham, MA, USA) to investigate the crystallinity and purity of catalysts. FT-IR analysis was studied by using the Nicolet FT-IR spectrometer (Waltham, MA, USA).

3.3. Catalyst Synthetic Procedure

3.3.1. Preparation of Ferrous Diselenide ($FeSe_2$)

Firstly, $FeCl_3$ (0.98 g, 6.1 mmol) and SeO_2 (3.2 g, 24.3 mmol) were dissolved in methanol (30 mL). Subsequently, pyridine (Py) (2.45 g, 31 mmol) was then added to the methanolic solution. The mixture was introduced into the glass-lined high-pressure reactor and filled with 2.5 MPa of CO at room temperature after purging with CO three times to remove air. The system was heated and stirred vigorously at a certain temperature. The reaction system was further charged with 8.3 MPa of CO at 160 °C and maintain during the reaction by using a gas reservoir. After the reaction, the solid part was filtered off and washed with MeOH (20 mL) for five times. The obtained catalyst was soxhleted with methanol in the reflux condenser for 8 h and dried under vacuum overnight. The obtained $FeSe_2$ was ground to get fine powder before applying to the reaction.

3.3.2. Preparation of 5 wt% $FeSe_2$ Supported on γ-Al_2O_3 ($FeSe_2/\gamma$-Al_2O_3)

The preparation of $FeSe_2/\gamma$-Al_2O_3 was similar for preparing $FeSe_2$ under otherwise identical conditions except for adding 3.1 g of dried γ-Al_2O_3 (γ-Al_2O_3 was firstly dried at 110 °C for 5 h) into the methanolic solution $FeCl_3$, SeO_2, and pyridine. The slurry was stirred for 30 min before introducing into the glass liner inside the high-pressure reactor.

3.4. Carbonylation Reaction

As a typical reaction, a carbonylation reaction was performed in a high-pressure reactor installed with a magnetic stirrer and electrical heater. The system was filled with CO (2.5 MPa) at room temperature after purging with CO three times to remove air and then heated to the required temperature with stirring. The system was further charged with 8.3 MPa CO at 160 °C and kept constant during the reaction using a gas reservoir equipped with a pressure regulator and a pressure transducer. After the reaction, the system was cooled to room temperature, followed by depressurization to unseal. The liquid sample obtained from the syringe filter was quantified using a gas chromatography installed with an HP-5 column (30 nm × 0.32 mm × 0.25 μm) and a flame ionization detector (FID), and a constant volume of heptane was added as a standard to calculate the yield of urethane. GC-Mass spectrometer and ^1H, ^{13}C NMR spectra (Bruker 300MHz NMR spectrometer) were used for the identities of products.

3.5. FT-IR Analysis of Carbonyl Selenide

3.5.1. Using O_2 as an Oxidant

The FT-IR experiment was performed in a high-pressure reactor by reacting 0.1 g of $FeSe_2$ with 8.3 MPa of a mixture gas of CO/O_2 (*v*/*v* = 80/20) in methanol (30 mL) as solvent at 100 °C. After 4 h reaction, the product was obtained by filtration and dried under vacuum for 12 h. The collected sample was pelletized with KBr and analyzed by the FT-IR spectrometer. The same procedure was also performed with $FeSe_2/\gamma$-Al_2O_3 and Se (0) metal.

3.5.2. Using Nitrobenzene (NB) as an Oxidant

A CO chemisorption study was performed using nitrobenzene (NB) as an oxidant instead of using oxygen. For this, 0.1 g of $FeSe_2$ was reacted with 8.3 MPa of CO in a high-pressure reactor with 1 equivalent NB to $FeSe_2$ in MeOH at 100 °C for 4 h. After the reaction, the sample was filtrated and vacuum dried for 12 h. The FT-IR analysis was conducted on the collected sample.

4. Conclusions

In this study, a remarkable yield of MPC was obtained via the reductive carbonylation of NB over a catalyst system consisting of $FeCl_3$, SeO_2, and Py, which appeared to be converted into a heterogeneous ferrous diselenide, $FeSe_2$. The $FeSe_2$ was impregnated onto γ-Al_2O_3 as support to synthesize a 5 wt%

$FeSe_2/\gamma$-Al_2O_3, which exhibited an impressive enhancement in terms of catalytic performance in the conversion of NB to MPC. The $FeSe_2/\gamma$-Al_2O_3-catalyzed carbonylation reaction was strongly affected by temperature and reaction time. The substituent at the para position of the aromatic ring has a significant impact on the yields of the corresponding carbamates, that is, the presence of the electron-withdrawing group at the para position tended to reduce the catalytic activity of the carbonylation reaction. Furthermore, the $FeSe_2/\gamma$-Al_2O_3 could be reused five times without a significant decrease in activity. Based on the FT-IR experiments on $FeSe_2$, it was likely to form asymmetric semi-bridging carbonyl diselenide, $FeSe_2$ (μ-CO) (**1b**) during the carbonylation, thus making it possible for the insertion of NB and complete the catalytic cycle, to regenerate **1b**. Moreover, a much higher yield of mono- and di-urethanes could be obtained through the $FeSe_2/\gamma$-Al_2O_3–catalyzed reductive carbonylation of a dual substrate system comprising nitro- and its corresponding amino-compound. The superiority of this $FeSe_2/\gamma$-Al_2O_3 catalyst is its low cost and simple preparation compared to the previously used noble metals such as Pd, Rh, and Ru for the reductive carbonylation of many different kinds of nitroarenes.

Supplementary Materials: The following are available online at http://www.mdpi.com/2073-4344/10/11/1228/s1, Figure S1: X-ray diffraction spectra (XRD) of standard Ferroselite $FeSe_2$, Figure S2: (a) X-ray diffraction spectra (XRD) of $FeSe_2/\gamma$ Al_2O_3, (b) XRD standard spectra of $Al_{2.144}O_{3.2}$ (γ - Aluminium oxide) PDF-number 79-1558-Cubic Fd-3m (227), Figure S3: EDX/EDS spectra of $FeSe_2$ and the atomic ratio calculation of Fe/Se, Figure S4: EDX/EDS spectra of $FeSe_2/\gamma$-Al_2O_3 and the atomic ratio calculation, Figure S5: X-ray photoelectron spectroscopy (XPS) survey spectra of $FeSe_2$, Figure S6: X-ray photoelectron spectroscopy (XPS) survey spectra of $FeSe_2/\gamma$ Al_2O_3, Figure S7: X-ray photoelectron spectroscopy (XPS) spectra of $FeSe_2$ in the region of (a) Fe3p, (b) Se3d, and (c) C1s, Figure S8: X-ray photoelectron spectroscopy (XPS) of $FeSe_2/\gamma$-Al_2O_3 in the region of (a) Fe3p and (b) Se3d, Figure S9: High resolution TEM images of (a) neat $FeSe_2$ prepared with the presence of pyridine, and (b) $FeSe_2/\gamma$-Al_2O_3 prepared with the presence of pyridine, Figure S10 Thermogravimetric analysis (TGA) of $FeSe_2$, Figure S11: GC-MS of the filtrate obtained in the reductive carbonylation reaction using $FeSe_2$ as catalyst with molar ratio NB/$FeSe_2$ = 1, Figure S12: GC-MS of the filtrate obtained in the reductive carbonylation reaction using $FeSe_2$ as catalyst with molar ratio NB/$FeSe_2$ = 4, Figure S13: 1H-NMR spectra of Methyl N-phenyl carbamate (MPC) product obtained from the reductive carbonylation rxn. 1H NMR (300 MHz, $CDCl_3$, δ 3.66 (s, 3H, OCH_3); 6.59 (s, 1H, NH); 6.95 (t, 1H, ArH); 7.17(m, 2H, ArH); 7.27 (d, 2H, ArH), Figure S14: ^{13}C-NMR of MPC product obtained from the reductive carbonylation reaction of nitrobenzene. ^{13}C NMR (300 MHz, $CDCl_3$, δ 52.5 (OCH_3); 118.85 (C_6H_5-); 123.6 (C_6H_5-); 129.1 (C_6H_5-); 137.9 (C_6H_5-); 154.19 (C_6H_5-), Figure S15: GC-MS of Methyl (4-methoxyphenyl) carbamate, Figure S16: GC-MS of Methyl (4-methylphenyl) carbamate, Figure S17: GC-MS of Methyl (4-bromophenyl) carbamate, Figure S18: GC-MS of Methyl (4-acetylphenyl) carbamate, Figure S19: GC-MS of Dimethyl toluene-2,4-dicarbamate, Figure S20: GC-MS of dimethyl 1,4-phenylenebiscarbamate, Figure S21: Scanning electron microscopy (SEM) figures of (a) fresh $FeSe_2/\gamma$-Al_2O_3 catalyst, and (b) spent $FeSe_2/\gamma$-Al_2O_3, Figure S22: X-ray diffraction spectra of (a) fresh catalyst $FeSe_2$, (b) recovered $FeSe_2$ after 5th recycling in the reductive carbonylation reaction of NB, Figure S23: XPS of the fresh and spent $FeSe_2/\gamma$-Al_2O_3 in the region of (a) Fe 3p; (b) Se 3d, Table S1: Different types of $FeSe_2$/support for the formation of MPC[a], Table S2: TON value of the reductive carbonylation reaction using $FeSe_2/\gamma$-Al_2O_3 as catalyst.

Author Contributions: Conceptualization, A.V.T., T.T.H.N. and Y.J.K.; methodology, A.V.T. and T.T.H.N.; validation, T.T.N., H.J.L. and J.B.; formal analysis, A.V.T. and T.T.H.N.; investigation, A.V.T. and T.T.H.N.; data curation, A.V.T.; writing-original draft preparation, A.V.T. and T.T.H.N.; writing-review and editing, A.V.T. and Y.J.K.; supervision, Y.J.K. All authors have read and agreed to the published version of the manuscript.

Funding: This study has been conducted with the support of the Korea Institute of Industrial Technology as "Development of eco-friendly production system technology for total periodic resource cycle (Kitech EO-20-0022)" and was funded by the Ministry of Science and ICT as "C1 Gas Refinery Program" (2015M3D3A1A01064895) through the National Research Foundation (NRF) of Korea

Conflicts of Interest: The authors declare no conflict of interest.

References

1. Kim, H.S.; Kim, Y.J.; Lee, H.; Lee, S.D.; Chin, C.S. Oxidative Carbonylation of Aromatic Amines by Selenium Compounds. *J. Catal.* **1999**, *184*, 526–534. [CrossRef]
2. Kim, H.S.; Kim, Y.J.; Bae, J.Y.; Kim, S.J.; Lah, M.S.; Chin, C.S. Imidazolium and Phosphonium Alkylselenites for the Catalytic Oxidative Carbonylation of Amines: Mechanistic Studies. *Organometallics* **2003**, *22*, 2498–2504. [CrossRef]

3. Kim, H.S.; Kim, Y.J.; Lee, H.; Park, K.Y.; Lee, C.; Chin, C.S. Ionic Liquids Containing Anionic Selenium Species: Applications for the Oxidative Carbonylation of Aniline. *Angew. Chem. Int. Ed.* **2002**, *41*, 4300–4303. [CrossRef]
4. Baba, T.; Kobayashi, A.; Kawanami, Y.; Inazu, K.; Ishikawa, A.; Echizenn, T.; Murai, K.; Aso, S.; Inomata, M. Characteristics of methoxycarbonylation of aromatic diamine with dimethyl carbonate to dicarbamate using a zinc acetate catalyst. *Green Chem.* **2005**, *7*, 159–165. [CrossRef]
5. Cenini, S.; Crotti, C.; Pizzotti, M.; Porta, F. Ruthenium carbonyl catalyzed reductive carbonylation of aromatic nitro compounds. A selective route to carbamates. *J. Org. Chem.* **1988**, *53*, 1243–1250. [CrossRef]
6. Ragaini, F.; Cognolato, C.; Gasperini, M.; Cenini, S. The carbonylation reaction of nitrobenzene to methyl phenylcarbamate: Highly efficient promoters for the palladium–phenanthroline catalytic system based on phosphorus acids. *Angew. Chem. Int. Ed. Engl.* **2003**, *42*, 2886–2889. [CrossRef]
7. Tafesh, A.M.; Weiguny, J. A review of the selective catalytic reduction of aromatic nitro compounds into aromatic amines, isocyanates, carbamates, and ureas using CO. *Chem. Rev.* **1996**, *96*, 2035–2052. [CrossRef]
8. Ferretti, F.; Gallo, E.; Ragaini, F. Mineral oil/methanol: A cheap biphasic reaction medium with thermomorphic properties and its application to the palladium-catalyzed carbonylation of nitrobenzene to methyl phenylcarbamate. *ChemCatChem* **2015**, *7*, 2241–2247. [CrossRef]
9. Mooibroek, T.J.; Schoon, L.; Bouwman, E.; Drent, E. Carbonylation of nitrobenzene in methanol with palladium bidentate phosphane complexes: An unexpectedly complex network of catalytic reactions, centred around a Pd-imido intermediate. *Chem. Eur. J.* **2011**, *17*, 13318–13333. [CrossRef]
10. Ferretti, F.; Gallo, E.; Ragaini, F. Nitrogen ligands effects in the palladium-catalyzed carbonylation reaction of nitrobenzene to give N-methyl phenylcarbamate. *J. Organomet. Chem.* **2014**, *771*, 59–67. [CrossRef]
11. Zhao, X.; Kang, L.; Wang, N.; An, H.; Li, F.; Wang, Y. Synthesis of Methyl N-Phenyl Carbamate Catalyzed by Ionic Liquid-Promoted Zinc Acetate. *Ind. Eng. Chem. Res.* **2012**, *51*, 11335–11340. [CrossRef]
12. Li, F.; Li, S.; Jia, A.; Gao, L.; Xue, W.; Zhang, Y.; Wang, Y. One-Pot Preparation of Methyl N-Phenyl Carbamate and Zn(OAc) 2/SiO2 Catalyst with Enhanced Stability. *ChemistrySelect* **2019**, *4*, 10581–10586. [CrossRef]
13. Ragaini, F. Away from phosgene: Reductive carbonylation of nitroarenes and oxidative carbonylation of amines, understanding the mechanism to improve performance. *Dalton Trans.* **2009**, *32*, 6251–6266. [CrossRef] [PubMed]
14. Wang, J.; Li, Q.; Dong, W.; Kang, M.; Wang, X.; Peng, S. A new non-phosgene route for synthesis of methyl N-phenyl carbamate from phenylurea and methanol. *Appl. Catal. A Gen.* **2004**, *261*, 191–197. [CrossRef]
15. Kang, M.; Zhou, H.; Tang, D.; Chen, X.; Guo, Y.; Zhao, N. Methyl N-phenyl carbamate synthesis over Zn/Al/Ce mixed oxide derived from hydrotalcite-like precursors. *RSC Adv.* **2019**, *9*, 42474–42480. [CrossRef]
16. Ma, Y.; Wang, L.; Yang, X.; Zhang, R. Enviromental-Friengly Synthesis of Alkyl Carbamates from Urea and Alcohols with Silica Gel Supported Catalysts. *Catalysts* **2018**, *8*, 579. [CrossRef]
17. Rojas-Buzo, S.; García-García, P.; Corma, A. Zr-MOF-808@MCM-41 catalyzed phosgene-free synthesis of polyurethane precursors. *Catal. Sci. Technol.* **2019**, *9*, 146–156. [CrossRef]
18. Zhang, Q.; Yuan, H.-Y.; Fukaya, N.; Yasuda, H.; Choi, J.-C. Direct synthesis of carbamate from CO2 using a task-specific ionic liquid catalyst. *Green Chem.* **2017**, *19*, 5614–5624. [CrossRef]
19. Sun, D.L.; Mai, J.J.; Deng, J.R.; Idem, R.; Liang, Z.W. One pot sythesis of Dialkyl Hexane-1,6-Dicarbamate from 1,6-Hexanediamine, Urea, and Alcohol over Zinc-Incorporated Berlinite (ZnAlPO4) Catalyst. *Catalysts* **2016**, *6*, 28. [CrossRef]
20. Choudary, B.M.; Rao, K.K.; Pirozhkov, S.D.; Lapidus, A.L. An efficient heterogenised palladium catalytic system for the reductive carbonylation of nitrobenzene to methyl N-phenylcarbamate. *J. Mol. Catal.* **1994**, *88*, 23–29. [CrossRef]
21. Bontempi, A.; Alessio, E.; Chanos, G.; Mestroni, G. Reductive carbonylation of nitroaromatic compounds to urethanes catalyzed by [Pd(1,10-phenanthroline)2][PF6]2 and related complexes. *J. Mol. Catal.* **1987**, *42*, 67–80. [CrossRef]
22. Cenini, S.; Pizzotti, M.; Crotti, C.; Ragaini, F.; Porta, F. Effects of neutral ligands in the reductive carbonylation of nitrobenzene catalysed by Ru3(CO)12 and Rh6(CO)16. *J. Mol. Catal.* **1988**, *49*, 59–69. [CrossRef]
23. Ferretti, F.; Formenti, D.; Ragaini, F. The reduction of organic nitro compounds by carbon monoxide as an effective strategy for the synthesis of N-heterocyclic compounds: A personal account. *Rend. Fis. Acc. Lincei* **2017**, *28*, 97–115. [CrossRef]

24. Ragaini, F.; Gasperini, M.; Cenini, S.; Arnera, L.; Caselli, A.; Macchi, P.; Casati, N. Mechanistic study of the Palladium–phenanthroline catalyzed carbonylation of nitroarenes and amines: Palladium–carbonyl intermediates and bifunctional effects. *Chem. Eur. J.* **2009**, *15*, 8064–8077. [CrossRef] [PubMed]
25. Shi, F.; He, Y.; Li, D.; Ma, Y.; Zhang, Q.; Deng, Y. Developing effective catalyst system for reductive carbonylation of nitrobenzene based on the diversity of ionic liquids. *J. Mol. Catal. A-Chem.* **2006**, *244*, 64–67. [CrossRef]
26. Macho, V.; Morávek, S.; Ilavský, J. Catalytic reductive carbonylation of nitrobenzene to methyl N-phenylcarbamate. *Chem. Pap.* **1991**, *45*, 363–368.
27. Wehman, P.; Borst, L.; Kamer, P.C.J.; van Leeuwen, P.W.N.M. Influence of an aromatic carboxylic acid as cocatalyst in the palladium-catalysed reductive carbonylation of aromatic nitro compounds. *J. Mol. Catal. A-Chem.* **1996**, *112*, 23–36. [CrossRef]
28. Kim, J.H.; Kim, D.W.; Cheong, M.S.; Kim, H.S.; Mukherjee, D.K. Catalytic activity of supported Rhodium(I) complex for the carbonylation of nitrobenzene: Mechanism for carbamate formation. *Bull. Korean Chem. Soc.* **2010**, *31*, 1621–1627. [CrossRef]
29. Alessio, E.; Mestroni, G. Catalytic reductive carbonylation of aromatic nitro compounds to urethanes promoted by supported palladium activated with 1,10-phenanthroline derivatives. *J. Organomet. Chem.* **1985**, *291*, 117–127. [CrossRef]
30. Wehman, P.; Dol, G.C.; Moorman, E.R.; Kamer, P.C.J.; van Leeuwen, P.W.N.M.; Fraanje, J.; Goubitz, K. Ligand effects in the Palladium-catalyzed reductive carbonylation of nitrobenzene. *Organometallics* **1994**, *13*, 4856–4869. [CrossRef]
31. Mooibroek, T.J.; Bouwman, E.; Drent, E. Mechanistic study of the L2Pd-catalyzed reduction of nitrobenzene with CO in methanol: Comparative study between diphosphane and 1,10-Phenanthroline complexes. *Organometallics* **2012**, *31*, 4142–4156. [CrossRef]
32. Cenini, S.; Ragaini, F.; Pizzotti, M.; Porta, F.; Mestroni, G.; Alessio, E. Carbonylation of nitrobenzene to phenyl isocyanate and methyl carbamate catalyzed by palladium and rhodium activated by chelating nitrogen donor ligands. *J. Mol. Catal.* **1991**, *64*, 179–190. [CrossRef]
33. Ragaini, F.; Cenini, S.; Fumagalli, A.; Crotti, C. [Rh(CO)4]−, [Rh5(CO)15]−, and bimetallic clusters as catalysts for the carbonylation of nitrobenzene to methyl phenylcarbamate. *J. Organomet. Chem.* **1992**, *428*, 401–408. [CrossRef]
34. Santi, R.; Romano, A.M.; Panella, F.; Santini, C. Palladium and silver reductive catalyzed carbonylation of nitrobenzene to methyl N-phenylcarbamate. *J. Mol. Catal. A-Chem.* **1997**, *127*, 95–99. [CrossRef]
35. Wehman, P.; van Donge, H.M.A.; Hagos, A.; Kamer, P.C.J.; van Leeuwen, P.W.N.M. Influence of various P/N and P/P ligands on the palladium-catalysed reductive carbonylation of nitrobenzene. *J. Organomet. Chem.* **1997**, *535*, 183–193. [CrossRef]
36. Gallo, E.; Ragaini, F.; Cenini, S.; Demartin, F. Investigation of the reactivity of palladium(0) complexes with nitroso compounds: Relevance to the palladium phenanthroline-catalysed carbonylation reactions of nitroarenes. *J. Organomet. Chem.* **1999**, *586*, 190–195. [CrossRef]
37. Ragaini, F.; Gallo, E.; Cenini, S. Promotion of the [PPN][Rh(CO)4]-catalysed carbonylation of nitrobenzene by 2-hydroxypyridine and related molecules: An apparent bifunctional activation. *J. Organomet. Chem.* **2000**, *593–594*, 109–118. [CrossRef]
38. Ferretti, F.; Ragaini, F.; Lariccia, R.; Gallo, E.; Cenini, S. New Nonsymmetric Phenanthrolines as Very Effective Ligands in the Palladium-Catalyzed Carbonylation of Nitrobenzene. *Organometallics* **2010**, *29*, 1465–1471. [CrossRef]
39. Kim, H.S.; Kim, Y.J.; Lee, H.; Park, K.Y.; Chin, C.S. The role of alkali metal carbonate on the SeO2-catalyzed oxidative carbonylation of cyclohexylamine and aniline. *J. Catal.* **1998**, *176*, 264–266. [CrossRef]
40. Besenyei, G.; Viski, P.; Simándi, L.I.; Nagy, F. Effect of water on the selenium catalyzed carbonylation of nitrobenzene to methyl N-phenylcarbamate. *React. Kinet. Catal. Lett.* **1984**, *24*, 293–296. [CrossRef]
41. Sonoda, N. Selenium assisted carbonylation with carbon monoxide. *Pure Appl. Chem.* **1993**, *65*, 699–706. [CrossRef]
42. Besenyei, G.B.; Viski, P.T.; Nagy, F.; Simándi, L.I. Catalytic carbonylation of nitrobenzene in the presence of selenium compounds. *Inorg. Chim. Acta* **1984**, *90*, L43–L44. [CrossRef]
43. Wang, X.; Li, P.; Yuan, X.; Lu, S. Selenium-catalyzed carbonylation of nitroarenes to symmetrical 1,3-diarylureas under solvent-free conditions. *J. Mol. Catal. A-Chem.* **2006**, *253*, 261–264. [CrossRef]

44. Wang, X.; Lu, S.; Yu, Z. Selenium-catalyzed carbonylation of nitroarenes to symmetrical 1,3-Diarylureas under atmospheric pressure. *Adv. Synth. Catal.* **2004**, *346*, 929–932. [CrossRef]
45. Kondo, K.; Yokoyama, S.; Noritaka, M.; Murai, S.; Sonoda, N. Reactions of Carbonyl Selenide with Amines and Aminoalcohols to Produce Ureas and Carbamates. *Angew. Chem. Int. Ed. Engl.* **1979**, *91*, 761. [CrossRef]
46. Tran, A.V.; Nguyen, T.T.; Lee, H.J.; Bae, S.W.; Baek, J.; Kim, H.S.; Kim, Y.J. CuSe2/CeO2 as a novel heterogeneous catalyst for reductive carbonylation of nitroarenes for generating urethanes. *Appl. Catal. A Gen.* **2019**, *587*, 117245. [CrossRef]
47. Huang, S.; He, Q.; Chen, W.; Zai, J.; Qiao, Q.; Qian, X. 3D hierarchical FeSe 2 microspheres: Controlled synthesis and applications in dye-sensitized solar cells. *Nano Energy* **2015**, *15*, 205–215. [CrossRef]
48. Ma, B.; Nie, Z.; Liu, C.; Kang, M.; Bardelli, F.; Chen, F.; Charlet, L. Kinetics of $FeSe_2$ oxidation by ferric iron and its reactivity compared with FeS2. *Sci. China Chem.* **2014**, *57*, 1300–1309. [CrossRef]
49. Zheng, Q.; Cheng, X.; Li, H. Microwave Synthesis of High Activity $FeSe_2$/C Catalyst toward Oxygen Reduction Reaction. *Catalysts* **2015**, *5*, 1079–1091. [CrossRef]
50. Jia, J.; Zhang, Q.; Li, Z.; Hu, X.; Liu, E.; Fan, J. Lateral heterojunctions within ultrathin FeS–$FeSe_2$ nanosheet semiconductors for photocatalytic hydrogen evolution. *J. Mater. Chem. A* **2019**, *7*, 3828–3841. [CrossRef]
51. Wehman, P.; Borst, L.; Kamer, P.C.J.; Leeuwen, P.W.N.M. Synthesis of functionalized carbamates through a palladium-catalyzed reductive carbonylation of substituted nitrobenzenes. *Chem. Ber.* **1997**, *130*, 13–21. [CrossRef]
52. Pearson, T.G.; Robinson, P.L. 83. Carbonyl selenide. Part I. Preparation and physical properties. *J. Chem. Soc.* **1932**, 652–660. [CrossRef]
53. Glemser, O.; Risler, T. Kohlenoxydverbindungen der nichtmetalle I darstellung und eigenschaften von carbonylselenid. *Z. Naturforschg B* **1948**, *3*, 1–6. [CrossRef]
54. Kondo, K.; Yokoyama, S.; Miyoshi, N.; Murai, S.; Sonoda, N. A new synthesis of carbonyl selenide. *Angew. Chem. Int. Ed. Engl.* **1979**, *18*, 691. [CrossRef]
55. Gómez Castaño, J.A.; Romano, R.M. Matrix isolation studies of carbonyl selenide, OCSe: Evidence of the formation of dimeric species, (OCSe)2. *Vib. Spectrosc.* **2014**, *70*, 28–35. [CrossRef]
56. Crabtree, R.H. *The Organometallic Chemistry of the Transition Metals*, 2nd ed.; John Wiley & Sons: New York, NY, USA, 1994; p. 487.
57. Cotton, F.A. *Metal Carbonyls: Some New Observations in an Old Field*; Lippard, S.J., Ed.; John Wiley & Sons: New York, NY, USA, 1976; Volume 21.

Publisher's Note: MDPI stays neutral with regard to jurisdictional claims in published maps and institutional affiliations.

© 2020 by the authors. Licensee MDPI, Basel, Switzerland. This article is an open access article distributed under the terms and conditions of the Creative Commons Attribution (CC BY) license (http://creativecommons.org/licenses/by/4.0/).